X-ray-absorption study of charge-density ordering in $(Ba_{1-x}K_x)BiO_3$

S. M. Heald and D. DiMarzio*

Materials Science Division, Brookhaven National Laboratory, Upton, New York 11973

M. Croft and M. S. Hegde

Physics Department, Rutgers University, Piscataway, New Jersey 08855

S. Li and M. Greenblatt

Department of Chemistry, Rutgers University, Piscataway, New Jersey 08855

Temperature-dependent x-ray-absorption measurements have been made on the Bi L_3 edge in $(Ba_{1-x}K_x)BiO_3$ with $x=0$ and 0.4. In the near-edge spectra there is clear evidence for Bi(6s) holes that depend on doping, but there does not seem to be a significant amount of Bi disproportionation into the 5+ and 3+ valencies in the undoped material. The extended x-ray-absorption fine-structure (EXAFS) measurements confirm previous diffraction studies of the structure and were also used to determine the EXAFS Debye-Waller factor for a number of Bi bonds. For $x=0$ the Debye-Waller factor differs strongly for the two types of Bi—O bonds, while for $x=0.4$ there is significant increase in the temperature-independent contribution. All of the temperature data could be fit well with an Einstein model, except for the Bi—O bond in a superconducting sample that showed a significant deviation from the expected behavior. These results, along with other considerations, are best explained by associating the charge-density ordering in the undoped material with holes on the O lattice and a tendency in the cubic superconducting sample towards the same type of charge-density-driven distortions.

I. INTRODUCTION

Interest in the $BiBaO_3$ system began with the discovery by Sleight et al.[1] that superconducting transition temperatures as high as 13 K can be obtained by replacing some of the Bi with Pb. The recent discovery of high-T_c superconductivity in Cu-O based systems[2-5] has renewed interest in other oxide superconductors. In the Cu-O systems it is now widely thought that the superconducting charge carriers in most materials are holes in the CuO_2 planes, which are a structural component of all of the compounds discovered to date.[6,7] The exact pairing mechanism for these holes is, however, still unknown. Whether a single pairing mechanism applies to both the Cu-O and Bi-O materials is a most important question in understanding the general phenomenon of high-T_c superconductivity.

Support for a single mechanism comes from the recent discovery that substitution of K for Ba in the parent $BaBiO_3$ compound results in transition temperatures as high as 30 K.[8] However, there are some differences between the Bi- and Cu-based compounds. The Cu-O compounds are all anisotropic, with conduction occurring predominantly in CuO_2 planes, while the K-doped Bi compounds are a simple-cubic perovskite. Also, the conduction states in the Bi compounds involve Bi(6s) and O(2p) states,[9] while in the Cu compounds it is the Cu(d) states which are interacting with the O(p) states. A number of authors[6,7,10] have emphasized the importance of magnetic interactions between the Cu(d) electrons and O(2p) holes in explaining the high T_c of the Cu materials,

but it appears a different mechanism must be operating in the nonmagnetic Bi system.[11] One suggestion is that charge-density waves (CDW) play an important role.[10,12,13] In the undoped material there is a strong breathing-mode lattice distortion, which has been taken as due to a disproportionation of the nominally Bi^{4+} into Bi^{3+} and Bi^{5+}.[14] These are the preferred valencies for Bi and such disproportionation could account for the semiconducting behavior of the undoped material. However, it has been pointed out that the CDW may actually reside on the oxygen sites.[10] For the doped material, more of the Bi should be driven toward Bi^{5+}, or alternatively, more holes are added to the O(p) band. This seems to break down the charge-density wave ordering on the Bi-O framework, freeing up the charge carriers and causing the material to be a conductor.

In this paper these questions are addressed by x-ray-absorption near-edge measurements on the Bi L_3 edge, and temperature-dependent measurements of the Bi extended x-ray-absorption fine-structure (EXAFS). The near-edge spectra depend sensitively on the chemical state of the atoms, and are used to determine the valency of the Bi atoms. We find similar behavior for the doped and undoped material with the amount of Bi(6s) holes, depending on formal valence. The extended fine structure is sensitive to structural parameters. A useful parametrization is the single scattering model

$$\chi(k) = \sum_j \frac{N_j A_j(k)}{R_j^2} e^{-2k^2\sigma_j^2} \sin[2kR_j + \Phi_j(k)] , \quad (1)$$

where k is the photoelectron wave vector, $A(k)$ and $\Phi(k)$ are overall amplitude and phase factors, respectively, N_j is number of atoms in shell j located at a mean distance R_j from the absorbing atom, and σ_j^2 is the mean-square variation of the bond length R_j. Since the structural parameters for these materials are well established, this paper will concentrate on the vibrational parameter σ_j^2 which can be determined from the temperature-dependent measurements. The combination of the EXAFS results and the near-edge data strongly support the view that the charge-density-wave distortion resides predominantly on the O sites.

II. EXPERIMENT

The $(Ba_{1-x}K_x)BiO_3$ samples were prepared from stoichiometric amounts of potassium, barium, and bismuth nitrates which were mixed together and calcined in air at 480 °C. The mixture was then thoroughly ground, heated for 3 h in helium gas at 780 °C, heated for 3 h at 480 °C in one atmosphere of oxygen, and slowly cooled to room temperature over a 3 h period. X-ray diffraction confirmed that the $x = 0.4$ material was single phase and had a cubic structure. The superconducting transition temperature from magnetic susceptibility measurements was 29 K.

As standard materials, the compounds Bi_2O_3, $Ba(Bi_{1-x}Tl_x)O_3$ with $x = 0.4$ and 0.5, and $NaBiO_3$ were measured. These have formal Bi valences of $3+$, $4.67+$, $5+$, and $5+$, respectively. The samples were prepared by rubbing fine powders onto scotch or kapton tape and stacking several layers to obtain the desired thickness. The measurements were made in transmission at beamline X-11A at the National Synchrotron Light Source (NSLS) using an Si(111) double-crystal monochrometer. The entrance slits were 0.2 mm, giving an energy resolution of about 2.7 eV. Energy calibration was checked by a simultaneous measurement of a Bi_2O_3 reference. In addition, the spectrum for a pure Bi metal sample was obtained by electron yield detection on a freshly abraded Bi surface. The temperature-dependent measurements were carried out using a Displex refrigerator with the sample temperature determined using an Fe-doped Au/Chromel thermocouple mounted directly on the Cu sample holder.

III. NEAR-EDGE RESULTS

The edge spectra for the $(Ba_{1-x}K_x)BiO_3$ materials are compared to Bi_2O_3 in Fig. 1(a). There is an observable shift to higher energy, as well as changes in the fine structure of the edge as compared to the $3+$ standard. Of particular interest is the small bump near the threshold. From the band-structure calculations, the low-lying states should consist of Bi(6s) and O(2p) states.[9] For the L_3 edge, dipole selection rules allow direct transitions to unfilled Bi s and d states. Thus, we believe that the low-lying feature is indicative of the amount of empty Bi(6s) states. For Bi^{3+} these states should be completely filled, and the existence of these features indicates the average Bi valence is greater than $3+$. Also, the valence is increasing with increasing K as expected.
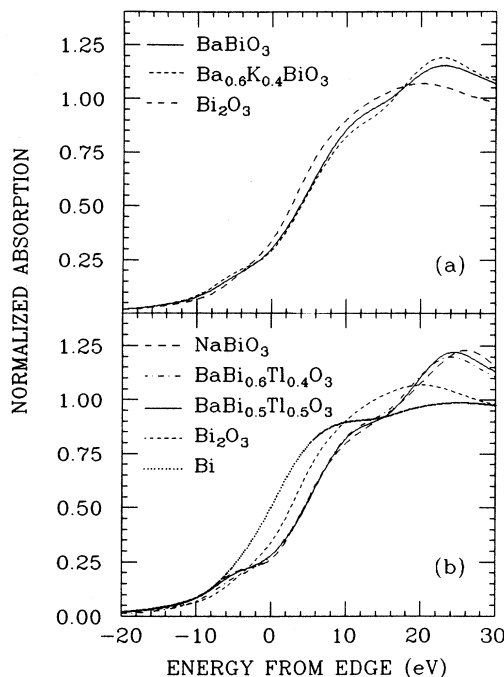

FIG. 1. Normalized x-ray absorption for (a) $Ba_{(1-x)}K_xBiO_3$ with $x = 0$ and 0.4 compared to Bi_2O_3, and (b) the standard compounds.

Support for this interpretation is shown in Fig. 1(b) in which the spectra for the standard materials are plotted. It is seen that the low-energy bump is largely absent in $Bi_2O_3(Bi^{3+})$, and strengthens with increasing formal valence. This is seen more easily in Fig. 2 which shows the derivative spectra for the low-energy region. It is clearly seen that the peak height depends on formal valence in a fairly monotonic fashion, and its magnitude for the superconductor is in good agreement with the standards.
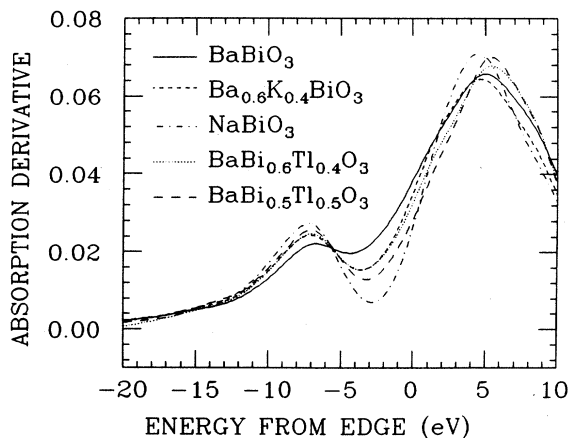

FIG. 2. Derivative of the spectra in Fig. 1 for the higher-valence compounds.

The position of the main part of the edge is less sensitive to the valence, with very few differences for all of the compounds with a formal valence greater than 3+. The edge positions for the $(Ba_{1-x}K_x)BiO_3$ components are slightly lower in energy than the high-valence standards, and are nearly independent of doping. There are, however, significant shifts in going from the metal to 3+, and from 3+ to greater than 3+. Such behavior is consistent with strong $O(2p)$-$Bi(6s)$ hybridization in the higher-valence compounds which is indicated by band-structure calculations. This covalency can result in the overall charge on a Bi site remaining relatively constant, as indicated by the edge position, even though the number of s holes is increasing. The main part of the edge should be dominated by transitions to d states, and some differences are observed. However, this part of the edge is also sensitive to structural changes. Since there are structural changes occurring, a detailed interpretation of these features is less certain without consideration of multiple-scattering processes.

The similarity of the edge structure from the doped and undoped samples indicates that the Bi environment in these materials is similar. Thus, either there is a disproportionation in both samples, or the charge-density distortion does not reside on the Bi sites. As shown below, the EXAFS results in combination with other considerations favor the latter interpretation. This conclusion is supported by x-ray photoemission (XPS) studies, which find a single set of Bi core levels.[15,16]

IV. EXAFS RESULTS

Figure 3 shows the EXAFS data obtained for the $x=0$ and 0.4 samples. High-quality data were obtained out to $k=16$ Å^{-1}. This meant that detailed analysis could be carried out on a number of atomic shells. Table I lists the calculated position of the first few shells in each compound. These are observed as strong peaks in the Fourier transformed data shown in Fig. 4. Since the structure of

TABLE I. Average coordination shells and their Einstein temperatures $(\Theta_E = h\nu_E)$ for Bi in $(Ba_{1-x}K_x)BiO_3$. The asterisk indicates an average distance is used for shells with bonds of different but similar distances.

	Shell	N	R (Å)	Θ_E (K)
$x=0$				
	Bi-O	3	2.120*	490(10)
	Bi-O	3	2.276*	338(10)
	Bi-Ba	8	3.766*	161(10)
	Bi-Bi	6	4.348*	
$x=0.4$				
	Bi-O	6	2.145	528(20)
	Bi-Ba	8	3.715	161(15)
	Bi-K			239(15)
	Bi-Bi	6	4.290	180(15)

$BaBiO_3$ seems to depend on the preparation procedure,[17] the first step in the analysis was a detailed examination of the Bi-O first shell in this material. Standard procedures based on the University of Washington program package were used in isolating the first shell $\chi(k)$ shown in Fig. 5. For the low-temperature data there is a strong beat near $k=8$, indicating that the shell is split into two distances. To determine the structural parameters for these two subshells, a two-shell fit was carried out using the program EXCURV86.[18] The theoretical phases were refined using the first shell data for the $x=0.4$ compound. This is composed of only a single distance, which can be well calibrated using x-ray diffraction data. The resulting first shell Bi-O distances were 2.11(0.01) and 2.28(0.01), in excellent agreement with Sleight and Cox.[14]

As seen in Fig. 5 the beating in the $x=0$ sample is strongly dependent on temperature, and is much reduced at 300 K. This indicates that at higher temperatures the contribution from one of the shells is strongly reduced such that its interference with the other shell is corre-
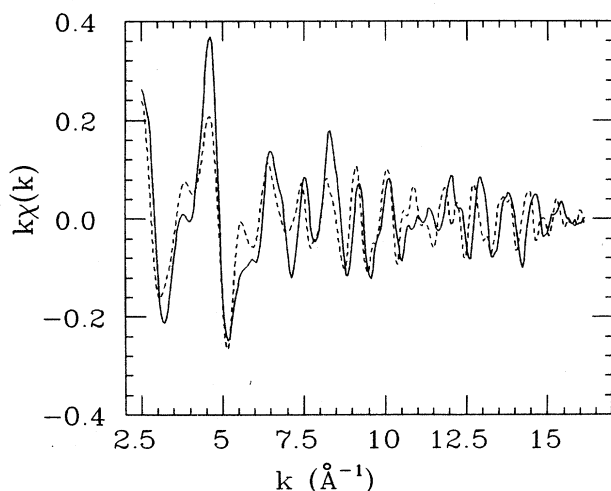

FIG. 3. EXAFS $k\chi(k)$ for the $x=0$ (dashed line) and $x=0.4$ (solid line) compounds.
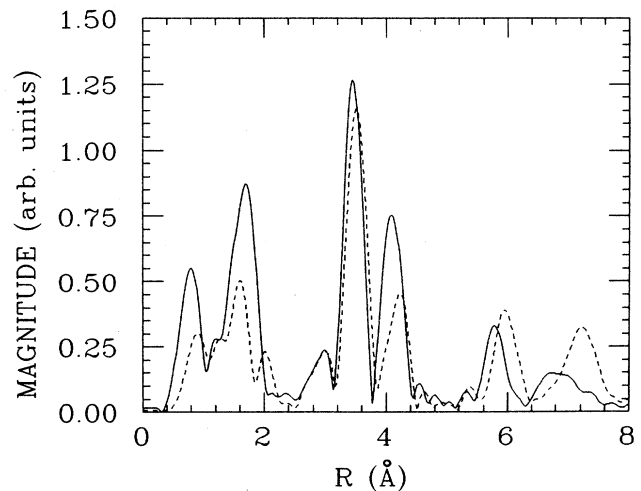

FIG. 4. Magnitude of the Fourier transform of $k\chi(k)$ for $x=0$ (dashed line) and $x=0.4$ (solid line).
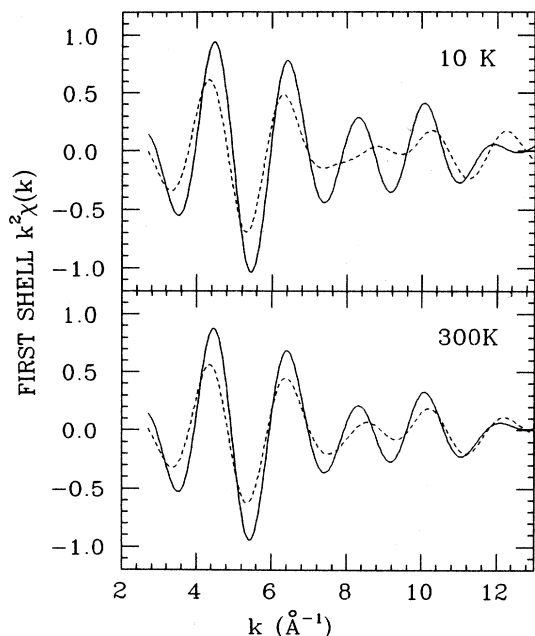
FIG. 5. Isolated first shell $k^2\chi(k)$ for $x=0$ (dashed line) and $x=0.4$ (solid line) at 10 and 300 K.

The Einstein model has been demonstrated to give a good estimate of the zero point σ^2 for many systems. It also should fit the temperature dependence well for harmonic systems. This is the case for the $x=0$ shells, although there is some scattering at low temperatures. For $x=0.4$ there is an indication of a small variation of σ^2 from the Einstein model in two separate temperature runs. In addition, upon comparison with the $x=0$ data, an additional temperature-independent disorder of 0.0025 $\mathring{A}^2$ was found for the doped material. This could be the result of structural disorder induced by the K substitution. However, for the Bi-Ba shell no additional disorder was found for the $x=0.4$ sample. In fact, the Bi—Ba bond for $x=0.4$ had a slightly smaller total σ^2 (by approximately 0.001 $\mathring{A}^2$) than the same bond in the undoped material.

Figure 7 shows the results of the analysis of the higher shells. These were obtained by the ratio method for the $x=0$ Bi-Ba and the $x=0.4$ Bi-Bi shells. For the $x=0.4$ Bi-Ba(K) shell the theoretical phases from EXCURV86 were used in a two-shell fit. To within the uncertainties, the results are all consistent with the Einstein fits. The corresponding Einstein temperatures are all summarized in Table I. Note that for $x=0$ we were unable to obtain σ^2 for the Bi—Bi bond due to strong interference from higher-shell Bi—O bonds. The values are quite reason-

spondingly reduced. To examine this behavior, fits were carried out for all of the temperature-dependent data to determine the Debye-Waller factor σ^2. These results are plotted in Fig. 6. The difference between the σ^2 results for the two bonds is quite striking, indicating that there are strong differences between the two sites. For $x=0.4$, the ratio method was used to determine σ^2, and the results are plotted in Fig. 7(a). The temperature dependence of σ^2 is similar to the shorter bond in the $x=0$ sample. In this case two different temperature runs were made, and the results are quite consistent.

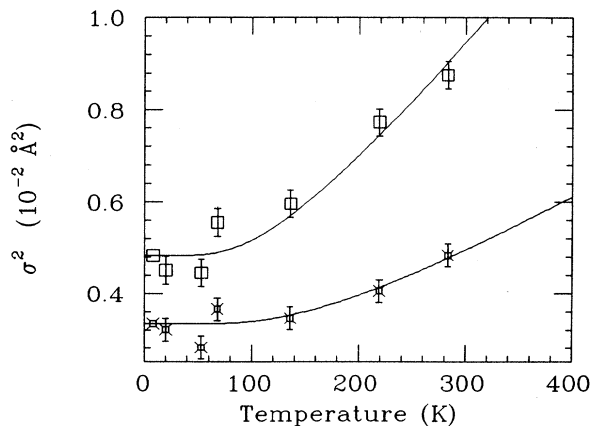The absolute scale in the σ^2 plots was determined from the Einstein model fits[19] plotted as lines in Figs. 6 and 7.

FIG. 6. Temperature-dependent σ^2 results for the $x=0$ 2.28 $\mathring{A}$ shell (squares) and the 2.12 $\mathring{A}$ shell (stars). The lines are Einstein model fits to the points.
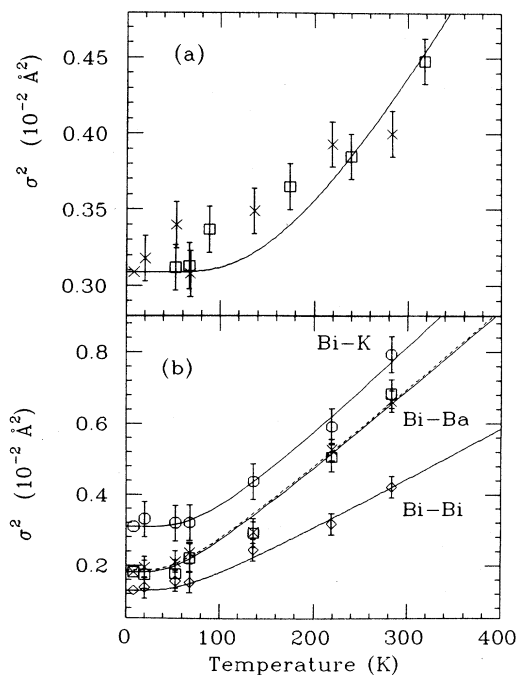

FIG. 7. (a) Temperature-dependent σ^2 results for the first shell (Bi-O) in the $x=0.4$ sample. The two symbols distinguish two separate experiments. In addition to the temperature-dependent contribution shown, there is an additional temperature-independent contribution of 0.0025 $\mathring{A}^2$. (b) Temperature-dependent σ^2 results for the higher shells indicated. The squares and the dashed line are for $x=0$ while the other data is for the $x=0.4$ sample.

able, and, in fact, are quite similar to the values found for the Cu-O superconductors.[20] Thus, with the possible exception of the Bi-O shell in the superconducting material, there is little indication of unusual behavior in the bonding of these compounds.

V. DISCUSSION AND CONCLUSIONS

From the ionic radii of the Bi and O atoms, the expected bond lengths for Bi(3+)—O and Bi(5+)—O are approximately 2.3 and 2.1 Å, respectively. The covalent radii give an intermediate length of 2.2 Å. Thus, the interpretation of disproportionation into 3+ and 5+ Bi for the undoped material is reasonable on the basis of bond lengths. However, for the superconducting material the EXAFS and diffraction data give only single Bi—O bond length that is intermediate between the 5+ and covalent values. This change in bonding is not accompanied by a significant edge shift. If disproportionation were occurring we would expect the main part of the edge to be at an intermediate position, and to change much more with doping than is observed. Thus, as holes are added with K doping, they are not going to the Bi sites, but rather to the O atoms.

There is some involvement of the Bi(6s) states as seen in the near-edge spectra. This represents the partially covalent nature of the Bi-O bonding. However, band-structure calculations for BaBiO$_3$ (Ref. 21) indicate that it is energetically favorable to add holes to the oxygen 2p states rather than the Bi(6s) states. Thus, we might expect most of the conduction-band holes to be associated with the O sites. As Emery[10] has pointed out, the energy cost of having two O(2p) holes per cell is probably fairly small since the wave function is spread out over six sites. In this picture it is more correct to associate the charge-density ordering in BaBiO$_3$ with the O lattice. This ordering opens up a gap in the conduction band leading to semiconducting behavior. Addition of holes through K doping immediately begins to change this ordering: first to an orthorhombic phase at $x = 0.04$ (Ref. 22) where each Bi has both long (2.22 Å) and short (2.11 Å) bonds, and then at higher concentrations to the cubic phase. Such behavior seems to be easier to understand in terms of different types of ordering of the holes on the O lattice, rather than mixed valency of the Bi atoms.

The EXAFS study found a significantly different value of σ^2 for the alternating Bi—O bonds in the undoped material. This is expected since the ordering of O(2p) holes should modify the bonding. For the superconducting material, both the temperature dependence of σ^2 and excess disorder argues against normal vibrational behavior. To further illustrate this, the total σ^2 is plotted in Fig. 8, assuming that the Bi—O bonds in the undoped material can be used as a standard (a reasonable assumption since they are well fit by the Einstein model). Two calculated curves are shown: the Einstein model which best fits the temperature dependence, and the model which gives the correct zero point σ^2. As can be seen, since the zero-point vibrational properties are related to bond strength, a simple harmonic model cannot be used to fit the total σ^2. Also, the absence of unusual behavior in the other
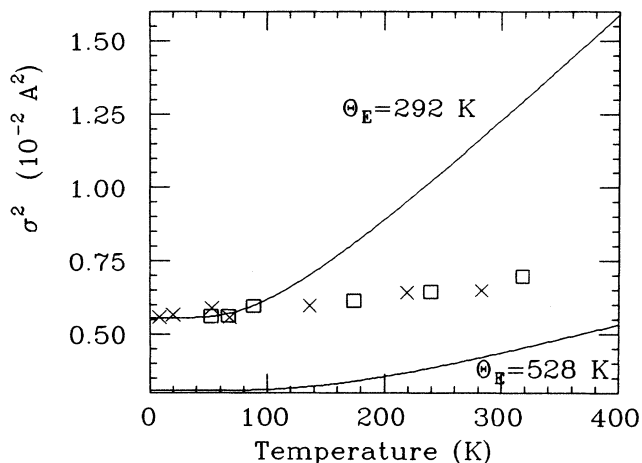

FIG. 8. The total Bi-O σ^2 for the $x = 0.4$ sample compared with two different Einstein models. The bottom curve ($\Theta_E = 528$) gives the best match to the temperature dependence, while the top curve ($\Theta_E = 292$ K) gives the best match to zero-temperature value.

bonds argues against an explanation of the temperature-independent part of σ^2 using structural disorder due to K doping. Diffraction studies[14,22−25] have found an anisotropic motion of the O atoms with a much larger motion perpendicular to the Bi—O direction. Such motion would not contribute strongly to the EXAFS σ^2, which is only sensitive to changes in the Bi—O bond length. This result was used to argue against a breathing-mode excitation as a dominant contribution to the electron-phonon coupling. However, in the undoped material the lattice distortion from cubic symmetry has both a breathing-mode component and a rotation of the Bi-O octahedra. It may be that a tendency towards this rotational distortion remains in the cubic $x = 0.4$ material. Either dynamic disorder or randomly distributed structural disorder would be consistent with the diffraction results.

Since the EXAFS measurements are not directly sensitive to these rotational modes, the effects in our measurements are weaker. The temperature-independent disorder observed in our measurements indicate that a substantial part of the rotational disorder may be built into the structure in a random fashion. This tendency towards the same type of lattice distortions found in the undoped material would be expected to modify the temperature dependence of the Bi-O σ^2, since there is likely to be coupling between these rotational modes and the breathing-mode distortions for which the EXAFS measurements are most sensitive. This could explain the observed deviations from harmonic behavior. Such distortions would not, however, strongly affect the behavior of the other nonoxygen containing bonds.

To summarize, the near-edge data along with other considerations indicate that a model invoking disproportionation into Bi(5+) and Bi(3+) for BaBiO$_3$ is oversimplified. While we observe an increase in Bi(6s)

holes with doping, the results are best explained by placing the majority of the holes predominantly on the O sites. For $x=0$, the EXAFS data confirm the previous diffraction results, and show a strong difference in the vibrational behavior of the two Bi—O bonds. For the superconducting sample, there are anomalies in the vibrational behavior of the Bi—O bond which may be related to rotation and breathing-mode distortions of the Bi-O octahedra. This tendency towards the charge-density ordering of the parent material may be involved in the pairing necessary for superconductivity.

[*]Current address: Grumman Corp. Res. Center, Bethpage, NY 11714.

[1]A. W. Sleight, J. L. Gillson, and P. E. Bierstedt, Solid State Commun. **17**, 977 (1976).

[2]J. G. Bednorz and K. A. Muller, Z. Phys. B **64**, 189 (1986).

[3]M. K. Wu et al., Phys. Rev. Lett. **58**, 908 (1987).

[4]H. Maeda, Y. Tanaka, M. Fukutomi, and T. Asano, Jpn. J. Appl. Phys. **27**, 1209 (1988).

[5]Z. Z. Sheng and A. M. Hermann, Nature **332**, 55 (1988).

[6]See Novel Superconductivity, edited by S. A. Wolf and V. Z. Kresin (Plenum, New York, 1987).

[7]T. M. Rice, Z. Phys. B **67**, 141 (1987).

[8]R. J. Cava et al., Nature **332**, 814 (1988).

[9]L. F. Mattheis and D. R. Hamman, Phys. Rev. Lett. **60**, 2681 (1988).

[10]V. J. Emery, IBM J. Res. Dev. **33**, 246 (1989).

[11]Y. J. Uemura et al., Phys. Rev. B **38**, 909 (1988).

[12]B. Battlogg, R. J. Cava, L. F. Schneemeyer, and G. P. Espinosa, IBM J. Res. Dev. **33**, 208 (1989).

[13]S. Pei et al., Phys. Rev. B **39**, 5767 (1989).

[14]D. E. Cox and A. W. Sleight, Acta. Crystallogr. B **35**, 1 (1979).

[15]M. W. Ruckman et al., Phys. Rev. B **39**, 7359 (1989).

[16]G. K. Wertheim, J. P. Remeika, and D. N. E. Buchanan, Phys. Rev. B **26**, 2120 (1982).

[17]C. Chaillout, J. P. Remeika, A. Santoro, and M. Marezio, Solid State Commun. **56**, 829 (1985).

[18]S. J. Gurman, N. Binsted, and I. Ross, J. Phys. C **17**, 143 (1984).

[19]E. Sevillano, H. Meuth, and J. J. Rehr, Phys. Rev. B **20**, 4908 (1979).

[20]C. Y. Yang et al., Phys. Rev. B **38**, 6568 (1988).

[21]L. F. Mattheiss and D. R. Hamann, Phys. Rev. B **28**, 4227 (1983).

[22]L. F. Schneemeyer et al., Nature **335**, 421 (1988).

[23]J. P. Wignacourt, J. S. Swinnea, H. Steinfink, and J. B. Goodenough, Appl. Phys. Lett. **53**, 1753 (1988).

[24]D. G. Hinks et al., Nature **333**, 836 (1988).

[25]G. H. Kwei et al., Phys. Rev. B **39**, 7378 (1989).